中國機械工程學刊第四十一卷第六期第 817~826 頁(民國一百零九年)
Journal of the Chinese Society of Mechanical Engineers, Vol.41, No.6, pp.817~826

Lubrication Analysis and Friction Loss Perdition of Main Bearings for Non-road Diesel Engines

Fen-Lian Huang*, Peng Wang**, Yu-Hua Bi***, Qian-Fan Xin* and Na Li**

Keywords：Main bearing; Elasto-hydrodynamic lubrication; Friction loss; Response surface methodology.

ABSTRACT

Based on the Greenwood /Tripp asperity theory and extended Reynolds equation under mass-conserving boundary condition, the elastic-hydrodynamic (EHD) mixed lubrication model of the main bearings according to the flexible engine was developed. The finite element models were reduced by component mode synthesis (CMS) method, and the validation is achieved by comparison with measurements from modal test. Then the oil film thickness, oil film pressure and friction power of each bearing under different operation conditions was calculated, and the validation of friction power is achieved by comparison with results obtained from motoring test with part of components decoupled from the engine. Finally, the friction loss prediction model of main bearings was established based on response surface methodology, and the influence of parameters were analyzed systematically through regression analysis method. The results show that with the increase of engine speed and oil viscosity, the friction power of main bearings become higher, and the bearing clearance made great effects on the friction loss.

Paper Received July,2019. Revised February,2020. Accepted July,2020. Author for Correspondence: Yu-Hua Bi.

** Ph.D., Yunnan Key Laboratory of Internal Combustion Engines, Kunming University of Science and Technology, Kunming 650500, China.*

*** Graduate Student, Yunnan Key Laboratory of Internal Combustion Engines, Kunming University of Science and Technology, Kunming 650500, China.*

****Professor, Yunnan Key Laboratory of Internal Combustion Engines, Kunming University of Science and Technology, Kunming 650500, China.*

INTRODUCTION

Main bearing is one of the key friction pairs of non-road diesel engine, which works under high temperature, heavy load and high-speed conditions (Lei, 2012). Its lubrication performances have become a core issue for reliable and low friction engine design. With the continuous strengthening in performance of diesel engine, the thermal and mechanical loads increase rapidly, which are exerted on the crankshaft and connecting rod mechanism. Accordingly, the crankshaft main bearings endure larger alternating loads and higher working temperature than ever, and their working conditions become more and more severe, and the lubrication problem become increasingly serious (Li, 2017). Friction loss is the main contributor to the mechanical loss and bearings are the major friction components.

Friction and lubrication in engines have long been the subject of tribological research and efforts to improve engine efficiency and durability. The experimental research of the bearings lubrication mainly focuses on the test of oil film thickness and axis orbit. Iran (1997) measured hydrodynamic lubricating oil film thicknesses in the middle main bearing of a heavy-duty diesel engine based on a capacitive measurement technique. Cheng (2003) used a kind of journal center locus measuring system to measure the oil film thickness, oil temperature, crank angle, speed, journal center locus and minimum oil film thickness of main bearing in diesel engine. Kataoka (2008) measured the oil film pressure in the main bearings of an operating engine using thin-film sensors.

Recent years, the simulation research of lubrication characteristics of main bearings has developed from static and dynamic analysis methods to multi-body dynamics and elastohydrodynamic lubrication theory. Kumar (1990) used the concept of mode-shapes for the transient elastohydrodynamic lubrication (EHD) analysis of journal bearings. Vijayaraghavan (1993) analyzed the dynamic performance of the Ruston and Hornsby VEB diesel engine connecting-rod bearing with circular and out-of-round profiles. Ye & Fu (2016) built a dynamic model of crankshaft and connecting rod mechanism and a hydrodynamic lubrication model of crankshaft main bearing based on the AVL-Designer software platform. Tong (2007) researched the lubrication of internal combustion engine (ICE)'s main bearing with considering thermal deformation effects based on the thermohydrodynamic lubrication theory of dynamically loaded bearing. Ruan (2017) studied the effects of engine block elastic deformation on the lubrication characteristics of main bearings. Zhang (1999) analyzed the effects of non-Newtonian shear thinning characteristics on dynamically loaded finite journal bearings in mixed lubrication. Wang & Wu (2012) used a finite-difference numerical model to analyze the influence of surface texture on lubrication performance of hydrodynamic journal bearing. Wang & Sun (2006) studied the lubrication performance of bearing system under different eccentricity radios, misaligning angles, surface roughness and surface pattern parameters.

With further research, more and more influencing factors have been considered in the numerical model, which makes the results of simulation increasingly close to the actual working conditions of crankshaft main bearings. Thus, the results of numerical simulation can provide better guidance for engineering design and optimization. In this study, considering rough contact, elastic deformation and oil filling rate, Vogel/Barus model as oil viscosity-temperature & pressure relationship, Reynolds equation with mass conservation boundary conditions couple with energy equation were solved by using AVL Excite multi-body dynamics analysis software. The power due to friction loss of the main bearings in multi-cylinder of non-road diesel engines were measured by motoring bench test. What's more, to predict the engine friction, the lubrication simulation data was analyzed using response surface methodology, which is a statistical analysis method used to quantitatively derive the factors affecting friction loss and the extent of their contribution, which is helpful to the design and optimization of crankshaft main bearing.

BASIC THEORY AND EQUATIONS

Extended Reynolds Equation

Considering the influence of bearing oil filling rate and surface roughness, we use the extended Reynolds equation in the form (Krasser, 1996):

$$-\frac{\partial}{\partial x}\left(\theta\cdot\alpha^2\cdot\frac{\partial p}{\partial x}\right)-\frac{\partial}{\partial z}\left(\theta\cdot\alpha^2\cdot\frac{\partial p}{\partial z}\right)=\frac{\partial}{\partial x}\left(\theta\cdot\beta\right)+\frac{\partial}{\partial \tau}\left(\theta\cdot\gamma\right), \quad (1)$$

with the Poiseuille term

$$-\alpha^2=h^3\cdot\int_0^y\rho\left(\int_0^y\frac{y'}{\eta'}dy'-\frac{\int_0^1\frac{y'}{\eta'}dy'}{\int_0^1\frac{1}{\eta'}dy'}\cdot\int_0^y\frac{1}{\eta'}dy'\right)dy, \quad (2)$$

the Couette term

$$\beta=h\cdot\left(u_j-u_s\right)\cdot\int_0^y\rho\cdot\left(1-\frac{\int_0^y\frac{1}{\eta'}dy'}{\int_0^1\frac{1}{\eta'}dy'}\right)dy, \quad (3)$$

and

$$\gamma=h\cdot\int_0^y\rho dy, \quad (4)$$

Where x is the circumferential bearing coordinate shell body fixed; z is axial bearing coordinate; y is radial bearing coordinate scaled with the clearance height h. This equation is solved for the hydrodynamic pressure p in the lubrication region and for the fill factor θ in the cavitation region, considering the bearings roughness and pressure boundary conditions at the bearing edge and at the oil supply position (oil bores and/or grooves) (Zhou, 2016).

Boundary conditions

The Reynolds equation is solved by the finite difference method, and the JFO boundary conditions is adopted to obtain the results. The boundary condition is expressed as follows:

(1) Axial boundary conditions:

$$p=p_a\left(z=\pm\frac{B}{2}\right), \quad (5)$$

(2) Periodic boundary conditions

$$p|_{\theta=0}=p|_{\theta=2\pi}, \quad (6)$$

(3) Cavitation boundary conditions

(a) Oil film rupture boundary

$$\frac{\partial p}{\partial x}=0,\ p=p_c, \quad (7)$$

(b) Oil film formation boundary

$$\frac{h^2}{12\eta}\cdot\frac{\partial p}{\partial x}=\frac{v_n}{2}\left(1-\theta\right), \quad (8)$$

(c) Cavitation region

$$p=p_c, \theta<1, \quad (9)$$

(c) Cavitation boundary

$$p=p_c, \theta=1, \quad (10)$$

(e) Cavitation region outside

$$p=p_{in}. \quad (11)$$

Oil Film Thickness

Considering the influence of the bearing elastic deformation and surface roughness on its lubrication characteristics, the oil film thickness is calculated by:

$$h(\theta) = h_{\min}(\theta) + \Delta h(\theta) + \delta h_p(\theta) + \delta h_T(\theta) + \sigma h(\theta) \, . \quad (12)$$

Bearing Dynamic Equation

The dynamic behavior of the crankshaft journal and shell are modelled separately from the oil film. The mathematical representation of the two bodies is derived from the equations of linear and angular momentum, resulting in the linear dynamic equation systems as follows (Chamani, 2015):

$$M_S \cdot \ddot{x}_S + D_S \cdot \dot{x}_S + K_S \cdot x_S = f_S^* \, , \quad (13)$$

$$M_J \cdot \ddot{x}_J + D_J \cdot \dot{x}_J + K_J \cdot x_J = f_J^* + f_J^a \, . \quad (14)$$

Viscosity Model

Viscosity dependence on pressure and temperature is calculated based on the classical Vogel/Barus equation (Wen, 2008):

$$\eta = \eta_0 \exp\left\{ \left(\ln \eta_0 + 9.67\right) \left[\left(1 + 5.1 \times 10^{-9} p\right)^{0.68} \left(\frac{T - 138}{T_0 - 138} \right)^{-1.1} - 1 \right] \right\} . \quad (15)$$

Density Model

Oil density dependence on pressure and temperature is calculated by Dowson Higginson formula:

$$\rho = \rho_0 \left(1 + \frac{0.6 \times 10^{-9} p}{1 + 1.7 \times 10^{-9} p} \right) \cdot \left[1 - 1 \times 10^{-4} \left(T - T_0 \right) \right] . \quad (16)$$

Energy equation

Within the Reynolds equation, both the oil film viscosity and density vary in three dimensions of space. For evaluation of these quantities, a thermal analysis must be carried out. The energy equation for the oil film considers heat convection in all directions, heat conduction in radial direction. Ignoring the effects of heat radiation, compression and viscous heating as well as heating caused by the asperity friction. And it is assumed that the temperature gradient along the film thickness direction is constant. This transient energy equation reads (Priebsch, 1996):

$$\rho c_p \left(\frac{\partial T}{\partial \tau} + u \frac{\partial t}{\partial x} + w \frac{\partial t}{\partial z} \right) = \eta \left[\left(\frac{\partial u}{\partial y} \right)^2 + \left(\frac{\partial w}{\partial y} \right)^2 \right] , \quad (17)$$

The boundary conditions for equation (17) are the continuity of the heat flow at the journal and shell surfaces and constant temperature at the oil supply (Zhou, 2016):

$$T\big|_{\theta=0} = T\big|_{\theta=2\pi} = T_{oil} \, , \quad (18)$$

$$\frac{\partial T}{\partial x}\Big|_{x=0} = 0 \, , \quad (19)$$

The journal is regarded as an isothermal body. At the boundary between lubricating oil and journal, there is

$$T = T_J \, . \quad (20)$$

Asperity Contact model

According to the Greenwood/Tripp theory (Greenwood,1970), a relation between force and stiffness is introduced, based on a statistic evaluation of the number of asperities in contact. The distribution of asperities' heights is regarded as Gaussian, and every peak contact is approximated by a Hertzian contact of a sphere, which radius is the mean summit radius. The asperity contact pressure is given by:

$$p_b(h) = KE^* F\left(4 - h/\sigma_s\right) , \quad (21)$$

When $\left(4 - h/\sigma_s\right) > 0$, it means the contact area is rough and mixed lubricating condition as running; when $\left(4 - h/\sigma_s\right) < 0$, it means the contact area is fully lubricated and bearings under hydrodynamic lubricating condition.

Power loss equation

The power loss includes the power consumption caused by hydrodynamic friction force and asperity friction force (Teng, 2016). The calculation formula is:

$$P_f = \left(\iint_A \left(\tau_H + \tau_A \right) \mathrm{d}\, x \, \mathrm{d}\, z \right) \omega R \, . \quad (22)$$

LUBRICATION SIMULATION

Main bearing lubrication model

We used the finite element software to build the main bearings and crankshaft three-dimensional solid models, used the component mode synthesis (CMS) method to build the rigid layer and dynamically reduce model. And the accuracy of the finite element simulation model was achieved by comparison simulation results with measurements. The specifications of engine and bearing are shown in Table 1. The EHD analysis flowchart is shown in Figure 1. The modal test of crankshaft and engine block is shown in Figure 2.

The comparison results of modal test are shown in Table 2. The error of the first five-order calculation modal and the test modal are less than 5%. The simulation modal shape agrees well with the experimental modal, indicating the finite element model is accurate. Then the reduced models were imported into the multi-body dynamics software AVL EXCITE, and the elastic hydrodynamic lubrication model was established based on the multi-body system dynamics theory. As shown in Figure 3.

Table 1. Specifications of engine and bearing.

Parameter	Value
Bore×Stroke	102×115 mm
Displacement	3.76 L
Cylinder Distance	124 mm
Maximum Gas Pressure	15.09 MPa
Maximum Torque	375N·m /1800 rpm
Rated Power	78 kW /2400 rpm
Main Bearing Width	35 (MB1\ MB5) mm, 30 (MB2-MB4) mm
Main Bearing Diameter	80 mm
Bearing Radius Clearance	0.035~0.077 mm
Oil Groove Position	270°~90°
Width of Oil Groove	4 mm
Main Journal Roughness	0.4μm
Oil Inlet Pressure	0.5 MPa
Oil Inlet Temperature	100℃
Cavitation Pressure	0.098 MPa
Oil Flow	10~15 L/min

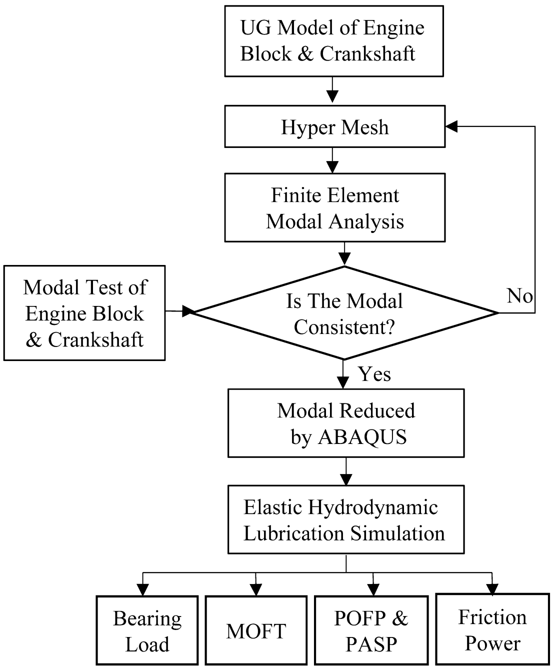

Fig. 1. EHD analysis flowchart.

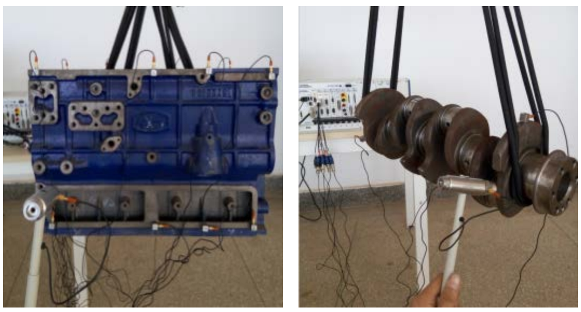
Fig. 2. Modal test process.

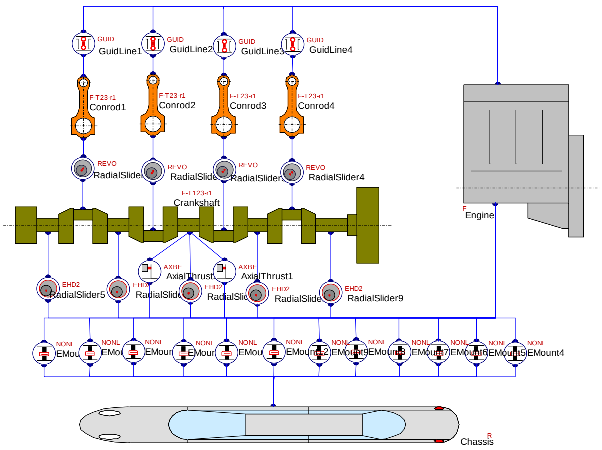

Fig. 3. Simulation model of crankshaft.

Table 2. Comparison modal test results.

Modal Degree	**Test (HZ)**	**Simulation (HZ)**	**Error**
1	249	258	3.6%
2	361	373	3.3%
3	598	612	1.6%
4	640	664	1.5%
5	748	773	3.3%

Simulation Results and Discussion

Based on the above theory and numerical model, the lubrication performances of five crankshaft main bearings in the 4-cylinder non-road diesel engine were respectively analyzed under three different speed conditions (Idle condition 800 rpm, Maximum torque condition 1600 rpm, Rated power condition 2400 rpm). This paper only takes No.5 main bearing as an example for analysis.

Cylinder pressure has significant effects on bearing force and minimum oil film thickness. We obtained the combustion gas pressure by bench test. The combustion gas pressure curve as a function of crank angle at each speed is shown in Figure 4.

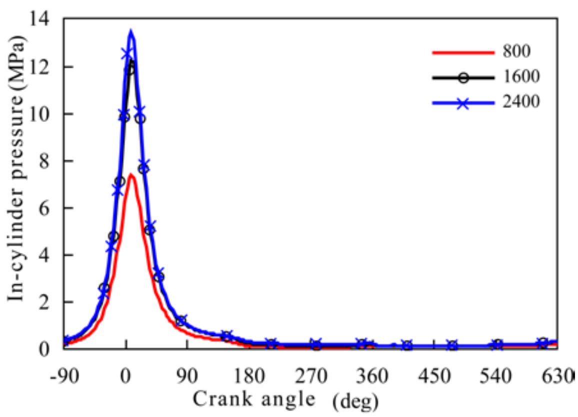

Fig. 4. Gas pressure in cylinder.

Minimum oil film thickness (MOFT) is a key indicator for determining the lubrication state of a bearing. Figure 5 shows the minimum oil film thickness of the No.5 main bearing as a function of crank angle. The analysis of figure 6 shows the valley value of the minimum oil film thickness occurs at 1097°CA (crank angle), a little behind the cylinder explosion. The minimum oil film thickness is generated under the maximum torque operation of 1600 rpm. The minimum oil film thickness of the No.5 main bearing is 0.65μm. The bearing surface roughness is 0.566 μm. Then we can calculate the critical value of the bearing elastic hydrodynamic lubrication is 0.566 μm~2.264 μm. According to the oil film thickness and surface roughness, the minimum film thickness ratio of No.5 main bearing is 1.15. It shows that the main bearing is in elastic hydrodynamic lubrication condition.

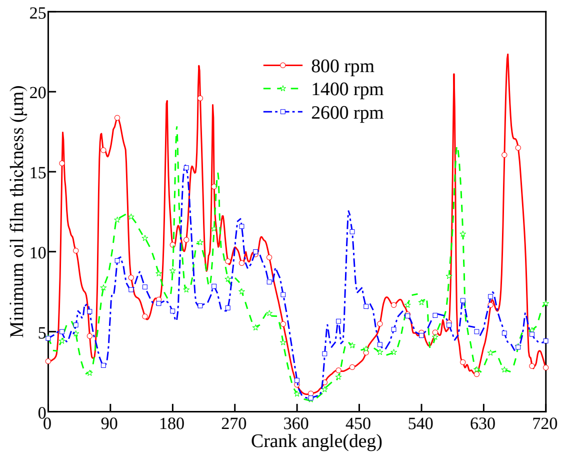

Fig. 5. Minimum oil film thickness.

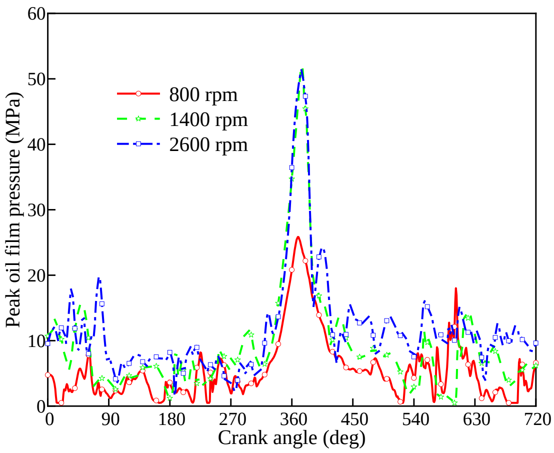

Fig. 6. Peak oil film pressure.

Figure 6 shows the relationship between the peak oil film pressure (POFP) and the crank angle. The maximum peak oil film pressure of the crankshaft main bearings rises accordingly with the increase of the engine speed. This results in the increase of maximum oil film pressure and the decrease of minimum film thickness in crankshaft main bearings. The maximum value appears at 1080°CA (crank angle) under the operating condition of 1600 rpm, the value is 51.98MPa.

Figure 7 shows the relationship between the peak asperity contact pressure (PASP) and the crank angle. The peak value of the rough contact pressure occurs at a maximum torque of 1600 rpm. This is because the maximum external load acting on the crankshaft main bearing is the largest under maximum torque condition, the maximum oil film pressure is the highest, the minimum film thickness is the thinnest under three speed conditions. The maximum peak asperity contact pressure value is 42.49 MPa, which is less than 50 MPa. It means no obvious eccentric wear occurred, and the lubrication performance of the bearing is fine.

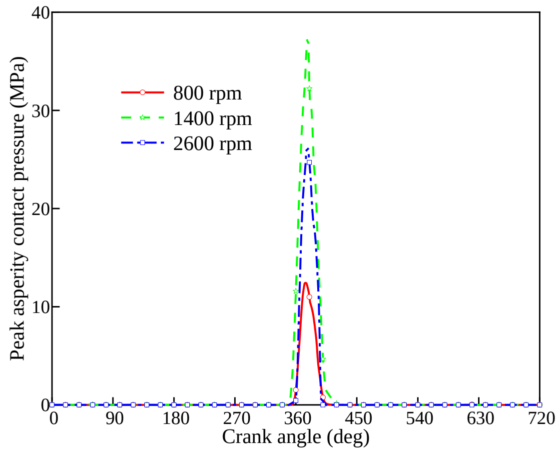

Fig. 7. Peak asperity contact pressure.

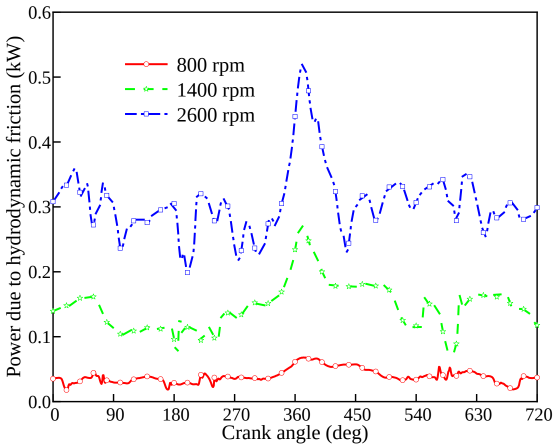

Fig. 8. Power due to hydrodynamic friction.

Figure 8 shows the variation of power due to hydrodynamic friction with crank angle. The hydrodynamic friction loss caused by the oil film pressure of crankshaft main bearings rise accordingly with the increase of the engine speed. Therefore, the lubrication performances of crankshaft main bearings under rate speed condition (2400 rpm) is relatively the severest among the three different speed conditions.

Figure 9 shows the variation curves of the power due to hydrodynamic friction plus asperity friction loss under different speed conditions. When the combustion gas pressure and external load acting on the crankshaft main bearing increases, the minimum oil film thickness relatively decreases, and the maximum oil film pressure and the friction power loss increase correspondingly. The hydrodynamic friction is the main contribution to power loss, and the friction loss caused by asperity contact is extremely small.

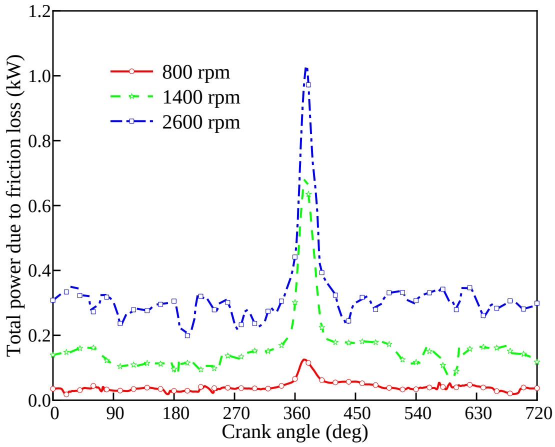

Fig. 9. Total power due to friction loss.

EXPERIMENTS

To estimate the power due to friction loss of main bearing at different speeds the following experiments had been performed.

Test Requirements

(1) The test was carried out on an AC electric dynamometer which can be dragged backward, and the torque is accurate to 0.05 N.m.

(2) Engine oil temperature accuracy of oil heater thermostat and external oil pump that can replace the engine oil pump were kept to ±1℃.

(3) Water temperature accuracy of water heater thermostat and external water pump that can replace the engine water pump were kept to ±1℃.

(4) Water temperature: 25/60/90℃.

(5) Engine oil temperature: 25/60/120℃.

(6) Engine speed: 500, 800, 1000～3600 rpm.

Test Methods

Without considering the influence of gas exchange, high temperature and high pressure in combustion chamber on the friction power. The components were gradually stripped to measure the friction loss of each part. The engine was motored by the AC dynamometer, the engine speed increased from low to high and then decreased from high to low during testing. The value of the two tests under the same speed should be in good agreement. If the difference is large, it needs to be retested. Mainly measured and recorded the speed, torque, oil pressure and temperature of main oil pipe, engine inlet water temperature and outlet pressure.

Test Results and Discussions

We removed the supercharger, water pump, oil pump, air compressor, fuel pump, valve train, camshaft drive gear, piston group and connecting rod group successively. The friction loss of the subsystem was obtained by comparing the difference before and after the removal. The results of motoring test are shown in Table 3. The friction power of the main bearing under the three operating conditions accounted for 6.95%, 9.91%, and 11.2% of the friction of the whole engine.

Table 3. friction power by motoring test.

Speed (rpm)	Whole engine (kW)	Crankshaft (kW)
800	3.02	0.21
1600	7.57	0.75
2400	15.01	1.68

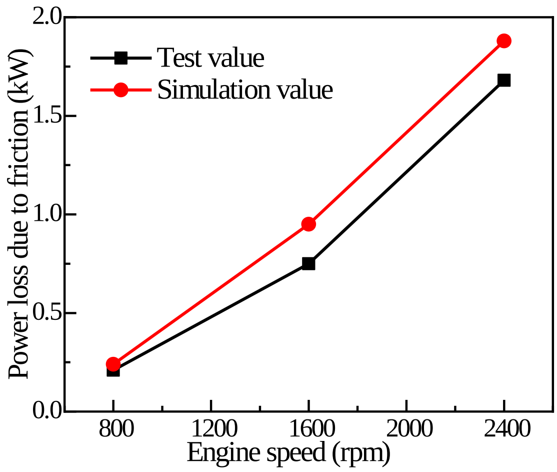

Fig. 10. Experiments vs. simulation results of crankshaft friction loss.

The comparison between the test value of friction power of the main bearing and the simulation results under different operating conditions is shown in Figure 10. The average relative error between the simulation results of the friction power and the test value under various operating conditions is 9.67%. The friction power of the main bearings measured by motoring test with disassembly method is lower than the simulation results.

PREDICTION OF FRICTION LOSS

Response surface methodology is an analysis method that models the relationship between characteristics and the causes through a polynomial approximation based on the test data. The model is then applied to understand the influence relationship and optimum conditions. The friction loss of the crankshaft bearing was studied by Box-Behnken test plan. We selected the engine speed, oil viscosity and bearing clearance as the factors, and each of the factors in table 4 had three levels.

Table 4. Factors and Level Values.

Factors	Levels	Code
A: Engine Speed (rpm)	800, 1600, 2400	-1, 0, 1
B: Oil Viscosity (MPa·s)	7.3, 9.6, 11.9	-1, 0, 1
C: Bearing clearance (μm)	32.5, 42.5, 52.5	-1, 0, 1

Friction Power Response Surface Modeling

By establishing a predictive regression model, the influence of key parameters (engine speed, oil viscosity, bearing clearance) and the coupling relationship between them on the frictional power of the main bearing was analyzed. Using Design export software, we set the test points according to Table 5 for the factors and levels of the main bearing, and then used the PU model to simulate the test points to obtain the friction loss power response. The results are shown in Table 6. Fitting the test results with quadratic linear regression and considering the first-order and second-order interactions, the predicted regression equation with the corresponding factors as the independent variables and the friction loss power as the dependent variable was obtained as follows:

$$\begin{aligned} Y &= 1.11 + 0.89A + 0.17B - 0.29C \\ &+ 0.14AB - 0.25AC - 0.056BC \end{aligned} \tag{23}$$

To ensure the accuracy and adaptability of the prediction model, it is necessary to carry out adaptive diagnosis and significant test on the regression model. The diagnosis results show that the regression model has a high correlation. The variance analysis and significance test data are shown in Table 6. When the probability *P* value is less than 0.05, it means that the model item is significant, and when the probability *P* value is greater than 0.1, the influence of the model item is not significant. Table 6 shows that the *P* values of *A*, *B*, *C*, *AB* and *AC* are less than 0.05, which is a significant factor; while the *P* value of *BC* is 0.2647, which is not significant. Then the prediction model is simplified as follows:

$$\begin{aligned} Y &= 1.11 + 0.89A + 0.17B - 0.29C \\ &+ 0.14AB - 0.25AC \end{aligned} \tag{24}$$

Table 5. Experimental Design.

NO.	*A*: Speed	*B*: Viscosity	*C*: Bearing Clearance	*Y*: Friction Power
1	2400	11.9	42.5	2.293
2	800	9.6	52.5	0.210
3	2400	7.3	42.5	1.640
4	800	11.9	42.5	0.292
5	800	9.6	32.5	0.300
6	800	7.3	42.5	0.212
7	1600	7.3	52.5	0.712
8	1600	11.9	52.5	0.921
9	1600	7.3	32.5	1.167
10	1600	11.9	32.5	1.601
11	2400	9.6	32.5	2.643
12	2400	9.6	52.5	1.543
13	1600	9.6	42.5	0.951

Table 6. Analysis of Variance.

Source	SS: Quadratic	MS: Mean Square	*F*	*P*: Probability
Model	7.57	1.26	148.97	<0.0001
A	6.31	6.31	774.83	<0.0001
B	0.24	0.24	27.94	0.0019
C	0.68	0.68	79.76	0.0001
AB	0.082	0.082	9.69	0.0208
AC	0.26	0.26	30.10	0.0015
BC	0.013	0.013	1.49	0.2647
Residual	0.051	8.472e-003		

Analysis of Main Bearings Response Surface

Figure 11 shows the correlation obtained through response surface methodology between individual factors and the Friction power.

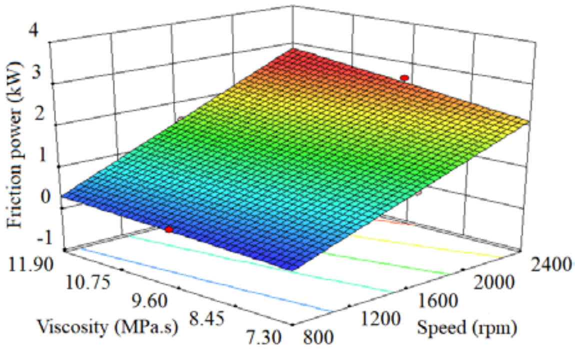

Fig. 11. Speed-viscosity response surface.

It can be seen from Fig. 11 that the influence of viscosity is more prominent at high speed. Under high-speed operating conditions, the temperature rising due to sliding continuously decreases lubricant viscosity on the sliding surface, thinning the oil film, causing the friction power due to asperity contact to increase. Therefore, when designing high power engine main bearings, the wear resistance of bearing bushes and lubricant cooling should be strengthened to reduce the friction power and wear of main bearings.

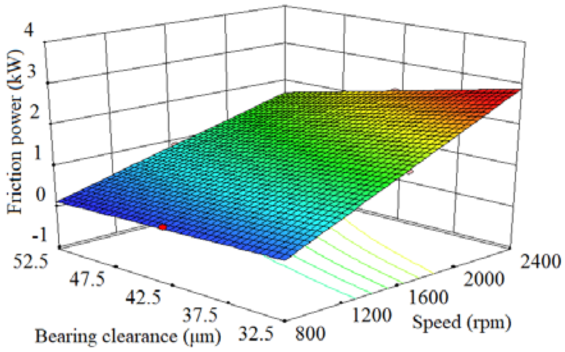

Fig. 12. Speed-bearing clearance response surface.

The relationship between the speed and the bearing clearance on the friction loss is shown in Figure 12. During low speed conditions, the bearing clearance has little effect on the friction power. During high speed conditions, the amount of oil passing through the sliding portion of the bearing varies with changes in oil pressure. When bearing clearance is small, the oil pressure and the amount of oil passing through is low, heat due to sliding continuously decreases lubricant viscosity on the sliding surface, thinning the oil film. For ensuring adequate oil flowing to bearings under normal working conditions, increasing bearing clearance appropriately will help to improve bearing lubrication.

CONCLUSION

(1) Diesel engine main bearing lubrication was affected by many factors. Computer simulation analysis based on the elastic hydrodynamic lubrication model could identify the lubrication performance and significant factors. A regression model of friction power was development based on response surface methodology, which can be applied to analyze the influence factors and predict the power due to friction loss.

(2) The average relative error between the simulation results of the friction power and the test value under various operating conditions is 9.67%. The friction power of the main bearings measured by motoring test with disassembly method is lower than the simulation results. That's because the in-cylinder pressure is consistent with the ambient pressure and there is no high-temperature gas in the cylinder during the motoring test. And after the moving parts are uninstalled, the inertial force and other loads of the remaining moving parts will change, and the lubrication of each friction pair will be different.

(3) Under high-speed operating conditions, the factor with the strongest effect on friction loss of crank main bearings are the oil viscosity and the bearing clearance. When designing high power engine main bearings, the wear resistance of bearing bushes and lubricant cooling should be strengthened, and the bearing clearance should be appropriately increased.

ACKNOWLEDGEMENT

Financial support for this work was provided by the Applied Basic Research Foundation of Yunnan Province (Item number: 2019FB073).

REFERENCES

Chamani, H., Karimaei, H., Bahrami, M., "Thermo-elasto-hydrodynamic (TEHD) analysis of oil film lubrication in big end bearing of a diesel engine", *Journal of Computational and Applied Research in Mechanical Engineering*, Vol. 1, No. 5, pp. 13-24 (2015).

Cheng, P, Gao, Y. and Han Y., "The Measurement of Journal Center Locus of the Main Bearing in Single-Cylinder Diesel Engine", *Chinese Internal Combustion Engine Engineering*, Vol. 24, No. 1, pp. 66-69 (2003).

Greenwood, J. A., Tripp, J. H., "The contact of two nominally flat rough surfaces", *Proceedings of the Institution of Mechanical Engineers*, Vol. 185, pp. 625-634 (1970).

Irani, K., Pekkari, M. and Hans-Erik Ångström., "Oil film thickness measurement in the middle main bearing of a six-cylinder supercharged 9 litre diesel engine using capacitive transducers", *Wear*, Vol. 207, No. 2, pp. 29-33 (1997).

Kumar, A., Goenka, P. K., Booker, J. F., "Modal Analysis of Elastohydrodynamic Lubrication: A Connecting Rod Application", ASME *Journal of Tribology*, Vol. 112, pp. 524-534 (1990).

Kataoka, T., Suzuki, Y. and Kato, N., "Measurement of Oil Film Pressure in the Main Bearings of an Operating Engine Using Thin-Film Sensors", *SAE Int. J. Engines*, Vol. 1, No. 1, pp. 352-358 (2009).

Krasser J., *Elastohydrodynamic analysis of dynamically loaded journal bearings*, Ph. D. thesis, Graz University of Technology, Graz, German (1996).

Li, N., Huang F. and Bi Y., "Study on Lubrication Characteristics and Influence Factors of Connecting Rod Big End Bearing for Non - Road Horizontal Diesel Engine", *International Powertrains, Fuels & Lubricants Meeting*, Beijing, China (2017).

Lei, J., Shen, L. and Bi, Y., "Analysis on influence factors of main bearing lubrication characteristics for horizontal diesel engine", *Transactions of the Chinese Society of Agricultural Engineering*, Vol. 28, No. 17, pp. 19-24 (2012).

Priebsch, H., Krasser, J., "Simulation of the Oil Film Behavior in Elastic Engine Bearings Considering Pressure and Temperature Dependent Oil Viscosity", *Tribology and Interface Engineering Series*, No. 32, pp. 651–659 (1996).

Ruan, D., Gao, Z. and Xu J., "Effects of engine block elastic deformation on the lubrication characteristics of main bearings", *Journal of Chongqing University*, Vol. 40, No. 1, pp. 1-9 (2017).

Tong, B., Gui, C., Sun, J., "Thermo-hydrodynamic lubrication analysis of internal combustion engine's main bearing considering thermal deformation effects", *Chinese Journal of Mechanical Engineering*, Vol.43, No. 6, pp. 180-185 (2007).

Teng, X., Zhang, J. and Ye, W., "Characteristic Analysis of Diesel Engine Main Bearing Lubrication Based on Thermo-elastic Hydrodynamic Pressure", *Ship Engineering*, Vol. 38, No. 4, pp. 61-64 (2016).

Vijayaraghavan, D., Brewe, D. E., Keith, T. G., "Effect of Out-of-Roundness on the Performance of a Diesel Engine Connecting-Rod Bearing", *ASME Journal of Tribology*, Vol. 115, No. 3, pp. 538-543 (1993).

Wang, Z., Sun, J., Gui, C., "Lubrication Performance Analysis of Misaligned Journal Bearing Considering Oil's Viscosity-Pressure Effect and Rough Surfaces", *Bearing*, Vol. 29, No. 12, pp. 4-7 (2006).

Wang, S. H., Wu, X. Y. and Zheng, J. H., "Influence of surface texture on lubrication performance of hydrodynamic journal bearing", *Applied Mechanics and Materials*, Vol. 120, pp. 426-431 (2011).

Wen, S., *Principles of tribology*. Tsinghua University Press, Beijing, China, (2008).

Ye, X., Fu, Y., Li, W., "Study on the Lubrication Performances of Crankshaft Main Bearings in a 16V Marine Diesel Engine", *International Powertrains, Fuels & Lubricants Meeting*, Beijing, China (2017).

Zhang, C., Zhang, Z., "Analysis of Crankshaft Bearings in Mixed Lubrication Including Non-Newtonian Effects", *Transactions of CSICE*, Vol. 17, No. 3, pp. 303-307 (1999).

Zhou, W., *Research on Simulation Analysis of Dynamic Characteristics and Bearing Lubrication Performance of High Speed and Heavy-Duty Diesel Engine Crankshaft*, Ph. D. thesis, Beijing Institute of Technology, Beijing, China (2016).

NOMENCLATURE

h oil film thickness (μm)

θ oil filling factor

η dynamic viscosity (Pa.s)

ρ oil density (kg/m^3)

u_j, u_s velocity of journal and shell (m/s)

B bearing width (mm)

p_c cavitation pressure (MPa)

p_{in} oil inlet pressure (MPa)

p_a atmospheric pressure (MPa)

v_n normal velocity of oil film boundary (m/s)

$\Delta h(\theta)$ difference between h and MOFT (μm)

$h_0(\theta)$ minimum oil film thickness (μm)

$\sigma h(\theta)$ film thickness variation due to roughness (μm)

$\Delta h_p(\theta)$ film thickness variation due to pressure (μm)

$\delta h_T(\theta)$ film thickness variation due to temperature (μm)

x_S , $\boldsymbol{x}_J$ displacement vector of shell and journal (m)

M_S, D_S, K_S mass, damping and stiffness matrix of shell

M_J, D_J, K_J mass, damping and stiffness matrix of journal

f_J^* journal contact forces and moments (N)

f_S^* shell contact forces and moments (N)

f_J^a external journal loads (N)

T_0 initial temperature of oil film (K)

T temperature of oil film (K)

c_p oil specific heat capacity (J/(kg·K))

u oil film velocities in circumferential direction (m/s)

w oil film velocities in axial direction (m/s)

p_b contact pressure (MPa)

E^* synthetical elastic modulus (N/m^2)

F oil film thickness function

σ_s synthesis surface roughness (μm)

R bearing radius (mm)

τ_H fluid shear stress (N/m^2)

τ_A shear stress of surface asperities (N/m^2)

非道路柴油機主軸承彈性流體動力潤滑分析及摩擦損失預測

黃粉蓮 王鵬 畢玉華 辛千凡 李 娜
昆明理工大學 雲南省內燃機重點實驗室

摘要

基於質量守恒邊界條件的廣義Reynolds 方程和Greenwood /Tripp 微凸體接觸理論，建立了柴油機主軸承彈性流體動力潤滑仿真模型，分析了柴油機不同工況下主軸承的載荷、油膜厚度、油膜壓力和摩擦功耗等變化規律。通過剝離法倒拖試驗，對整機和主軸承的摩擦損失進行測量。基於響應曲面法分析了發動機轉速、機油粘度、軸承間隙對主軸承摩擦功耗的影響規律。